Fracture Mechanics of Concrete and Concrete Structures -
Recent Advances in Fracture Mechanics of Concrete - B. H. Oh, et al.(eds)

Fracture toughness of hydrated cement paste using nanoindentation

M. Reda Taha, E. Soliman, M. Sheyka, A. Reinhardt & M. Al-Haik
University of New Mexico, Albuquerque, NM, USA

ABSTRACT: Nanoindentation has been reported as an effective tool for realizing the strength and stiffness (modulus of elasticity) of different materials including cementitious composites. However, to the best of the authors' knowledge, nanoscale fracture of cementitious materials has rarely been examined. Fracture of cementitious composites has been typically studied by observing crack growth of notched macroscale specimens subjected to flexural or tension loads. We discuss the possible characterization of fracture toughness of cementitious composites using contact mechanics at the nanoscale. This paper reports on the first experiments to evaluate fracture toughness of hydrated cement paste at the nanoscale. The analysis method is based on evaluating the energy absorbed by radial cracks propagating from the indentation imprint in brittle materials. Nanoindentation experiments performed using Berkovich nanoindenter are reported. The hardness, reduced elastic modulus and fracture toughness of hydrated cement paste are extracted from nanoindentation experiments. Fracture toughness is evaluated using an equivalent elastic crack energy approach and is compared to macroscale fracture toughness of hydrated cement paste from the literature. The use of nanoindentation for evaluating fracture toughness of concrete constituents might help shedding light on the spatial distribution of fracture toughness in homogenized concrete matrices and the contribution of the different microstructural phases to fracture of concrete.

1 INTRODUCTION

1.1 *Background*

Concrete is a heterogeneous composite. It is believed that developments to further enhance concrete performance require robust understanding of the role played by the different nanoscale phases that make the cementitious composite. Contemporary research has shown that concrete's various material properties such as its elastic modulus, energy absorption and creep compliance can be extracted at the nanoscale from instrumented nanoindentation (Fisher-Cripps 2004). Researchers have shown nanoindentation to be a successful method for classifying microstructural phases such as low density (LD) and high density (HD) calcium silicate hydrates (CSH) (Constantinides & Ulm 2004). Researchers have displayed the ability to obtain hardness and reduced modulus of microstructural phases of cementitious materials (Mondal et al. 2007). Nanoindentation was also proven capable for characterizing the significance of admixtures such as nanosilica and carbon nanotubes on cementitious materials strength and stiffness (Li et al. 2007, Kim et al. 2010).

There has also been a growing interest in identifying fracture toughness parameters of different materials using nanoindentation (Scholz et al. 2004). To the best of the authors' knowledge, such analysis has not been applied to cementitious materials yet. The major challenge in determining fracture toughness of materials using nanoindentation is the difficulty to obtain robust measurements of submicron crack propagation as the stress increases.

There have been some suggestions of post-measurement of the crack length extended from the edge of the indentation impression after unloading. This measurement can be determined using optical microscopes or atomic force microscope (AFM). Such measurements have been shown possible with metallic and thin film specimens (Li et al. 1997). However, there is considerable difficulty to obtain these measurements from cementitious composites with the multiple cracking in the cement paste. Moreover, stable propagation of radial cracks, or what is known as picture-frame cracks, under nanoindentation load has been questioned by many researchers (Chen & Bull 2007) and is a function of the material examined. This concept will be discussed below. A robust method for determining fracture toughness from nanoindentation can be based on energy assumptions independent of measuring radial crack propagation.

1.2 *Nanoindentation*

The main goal of the nanoindentation experiments is to establish the load-nanoindentation displacement curves to allow extracting the material hardness (H)

and modulus of elasticity (E) from these load displacement curves (Fisher-Cripps 2004). Figure 1 shows a typical load indentation curve for an elastic-plastic material (hardened tool steel) tested in the authors' laboratory.

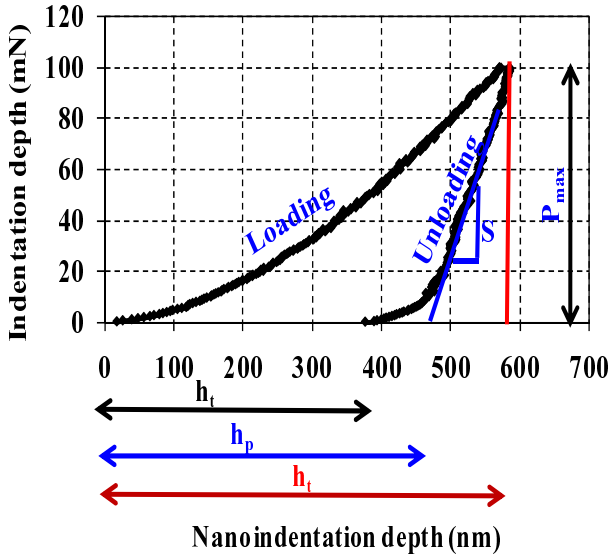

Figure 1. Typical load-nanoindentation curve for hardened tool steel. The curve shows loading and unloading curves used to extract the mechanical properties of the material.

In Figure 1, P_{MAX} is the maximum indentation load and h_t and h_r are nanoindentation depths corresponding to the applied load obtained from the nanoindentation test. The parameters S and h_p can be obtained by examining the upper portion of the unloading curve. Nanoindentation analysis by Oliver & Pharr (1992) realized a curvature in the upper portion of the unloading curve through indentation of six different types of materials with a Berkovich indenter. To account for the nonlinearity in the unloading curve Oliver and Pharr suggested curve fitting with a power law function. This work was done with a Berkovich indenter but the method can be applied to other indenters (Oliver & Pharr 1992).

Once this relationship describing the upper portion of the unloading curve is established, the slope, S, can be determined as the slope at P_{MAX}. The plastic depth h_p can then be calculated as

$$h_p = h_t - \varepsilon \frac{P_{MAX}}{S} \tag{1}$$

where $\epsilon = 0.72$ for a conical indenter, $\epsilon = 0.75$ for a Berkovich and spherical indenters, and $\epsilon = 1$ for a flat punch indenter (Fisher-Cripps 2004). The projected area of indentation (A) can be calculated. The area function differs with indenter type. Equation 2 gives the area function for a Berkovich indenter.

$$A = 24.5 h_p^{\,2} \tag{2}$$

Indentation hardness (H) is calculated as the stress induced by the maximum load over projected area

$$H = \frac{P_{MAX}}{A} \tag{3}$$

The reduced modulus, (E_r) which is often considered equivalent to Young's modulus, is obtained from Equation 4 (Oliver & Pharr 1992).

$$E_r = \frac{\sqrt{\pi}}{2} \frac{S}{\sqrt{A}} \tag{4}$$

By fitting relationships to describe the loading (P_L) and unloading (P_{UL}) curves as a function of indentation depth h, elastic (U_e), the total (U_t), and plastic (U_p) energies can be obtained from Equations 5, 6 and 7 respectively.

$$U_e = \int_{h_r}^{h_{MAX}} P_{UL}\, dh \tag{5}$$

$$U_t = \int_{0}^{h_{MAX}} P_L\, dh \tag{6}$$

$$U_p = U_t - U_e \tag{7}$$

It is important to note that most fracture toughness analysis methods using instrumented indentation have been developed for brittle or ductile materials with clear plasticity. In quasi-brittle materials like cement paste, cracking represents the major source of plasticity. We note that in the case of quasi-brittle materials such as cementitious composites, the plastic energy includes the energy consumed in radial crack propagation and in forming the fracture process zone at the crack tip. This issue will be further discussed in the Methods section below.

1.3 *Fracture toughness using instrumented indentation*

Harding et al. (1995) suggested using a technique in which the fracture toughness of thin films was calculated from nanoindentation load displacement data. The method is based on the radial cracking that ensues after a sharp indenter such as a Berkovich or Vickers indenter encounters a brittle material. This method was developed and applied using Vickers microindentation where large cracks in the range of 100 μm in length were produced using loads of 1000 gm. The fracture toughness K_c was derived as a

function of other material properties including its elastic modulus, E, hardness, H, and the geometry of the indentation with the load:

$$K_c = \alpha\left(\frac{E}{H}\right)^n\left(\frac{P}{c^{3/2}}\right) \tag{8}$$

where, P is the applied indentation load, α is an empirical constant that is related to the geometry of the indenter used and c is the radial crack length corresponding to the applied load as shown in Figure 2.

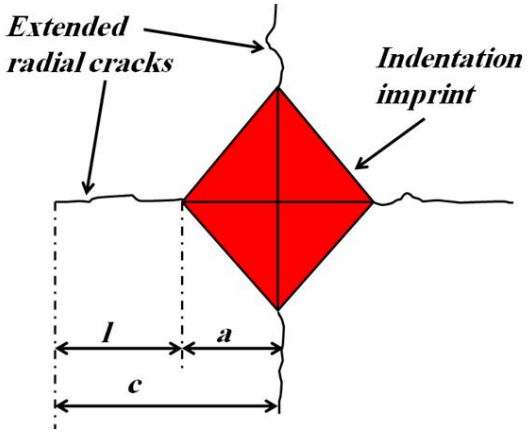

Figure 2. Geometrical relationship showing the relation between the extended radial cracks and the indentation imprint in Vickers indentation after Harding et al. (1995).

The above method worked poorly for determining fracture toughness of thin films due to the limited level of radial cracking. Harding et al. (1995) proposed using a sharper indenter, called the corner cube indenter, to increase radial cracking. This indenter has an angle between the axis of symmetry of 35.3° compared to 65.3° of the Berkovich indenter. The corner cube indenter showed acceptable results. Previous research showed that the $P/c^{3/2}$ in Equation 8 is a constant for a given material. Anstis et al. (1981) determined α and n to be 0.0098 and 2/3 respectively while Dukino & Swain (1992) showed the values of α and n to be 0.016 and 0.5 respectively. Laugier (1987) proposed another expression for relating radial crack propagation to fracture toughness as:

$$Kc = xv\left(\frac{a}{l}\right)^{1/2}\left(\frac{E}{H}\right)^{2/3}\left(\frac{P}{c^{3/2}}\right) \tag{9}$$

where xv is 0.015 and a and l relate to Figure 2. The two methods are then used for comparison between fracture toughness values. Experimental comparison between fracture toughness extracted from Vickers and Berkovich indenters while accounting for the difference in the number of radial cracks: 4 for Vickers and 3 for Berkovich, showed that fracture toughness values extracted from Berkovich indentations were more consistent.

Another interesting approach looked at determining the fracture toughness considering energy conservation. For instance, Rosenfeld et al. (1990) developed an analytical model to determine the mixed mode interfacial fracture toughness of epoxy coatings on soda-lime glass substrates using Vickers' micro-indentation. The method is based on computing the strain energy consumed in annular plate located above the crack using mechanics of materials. The elastic energy release rate can then be calculated by differentiating the energy with respect to the crack area. Field et al. (2003) computed the fracture toughness based on pop-in penetration. Pop-in occurs due to a change in crack morphology when the median crack nucleates and propagates upward at the boundary of plastic zone to join the existing radial cracks. This results in extra penetration at the same indentation load level. The pop-in effect becomes negligible in materials whose microstructures contain a distribution of voids in various sizes because the pop-in effect due to these voids would dominate.

Chen & Bull (2007) studied the fracture in thin optical coating on glass. Experiments on glass showed that well-developed radial cracks might not be observed when indenting thin films. This is contrary to the case of indenting a bulk material where the radial cracks are well-developed and in some cases measurable. Therefore, an energy approach to estimate the fracture toughness was proposed. The proposed approach takes into account the effect of through thickness fracture. The total energy during indentation can be decomposed to elastic, plastic, fracture and other negligible energies. The total and elastic energies can be computed from the nanoindentation load-penetration curve. The plastic energy can be computed as the difference between the elastic and total energy. Cheng et al. (2002) suggested computing the plastic energy as a function of the residual to total penetration ratio using the following Equation 10.

$$\frac{W_p}{W_t} = (1+\gamma)\frac{h_f}{h_m} - \gamma \tag{10}$$

W_p is the plastic work, W_t is the total work, h_f is the residual penetration, h_m is the maximum penetration, and γ is constant dependant on the indenter geometry. Once the plastic work is computed, the fracture energy (U_f) can be computed as the difference between plastic energy and plastic work. Thus, the fracture toughness can be computed as

$$K_{IC} = \sqrt{\frac{U_f E}{\left(1-\upsilon^2\right) A_{fra}}} \tag{11}$$

$$A_{fra} = \frac{3a^2}{2s} t \tag{12}$$

A_{fra} is the total interfacial fracture area of the picture frame cracks, a is the radial dimension of the indentation, s is the spacing between the lateral cracks, t is the thickness of the specimen as shown in Figure 3.

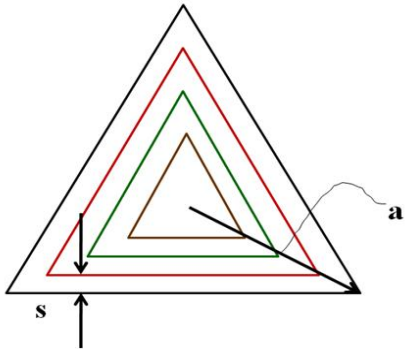

Figure 3. Schematic of the picture-frame crack geometry induced by a Berkovich indenter after (Chen & Bull 2007).

The above discussion highlights some of the basic research on the field of determining fracture toughness using instrumented indentation. Other methods that combine the finite element method and experimental measurements have also been suggested (Cheng et al. 2002). A detailed review of the different approaches for computing fracture toughness from indentation measurements might be found elsewhere for space limitations (Reda Taha et al., in prep.). We discuss below the application of the energy approach to extract fracture toughness for cement paste using nanoindentation.

2 EXPERIMENTAL METHODS

The specimens used for nanoindentation were cement paste specimens produced using 0.5 water/cement ratio. The nanoindentation tests were performed using an instrumented nanoindenter (NanoTestTM 600 indenter platform from Micro Materials, Inc., Wrexham, UK). Nanoindentations were performed using a Berkovich nanoindenter. The indenter tip was attached to a pendulum mounted vertically to a frictionless pivot. For loading, an electrical current was passed through an electromagnetic coil mounted at the top of the pendulum. The current creates an attraction between the coil and a stationary magnet mounted parallel to the coil. This attraction and motion caused the pendulum to rotate about a frictionless pivot and displace the indenter into the vertically mounted sample. The displacement of the nanoindenter tip was then measured and recorded at a nanoscale resolution by a sensitive capacitive transducer.

Nanoindentation experiments were performed on the cement paste specimens after 28 days of curing in a standard water-lime bath (23 °C). The specimens were extracted from the bulk cement paste specimens by slicing 25.4 mm x 25.4 mm x 25.4 mm cubes with a diamond blade saw. The specimens were then cast in a fast-set acrylic epoxy. After the epoxy hardened, the sample surfaces were ground with a mechanical polishing wheel with a grit size of 120 for a total of ten minutes. Then the sample surfaces were ground with grits of 240, 600, 1000, 1500 and 2000 in respective order for a total of 5 minutes at each scale. The reason for extended grinding at the 120 grit level was to ensure an even surface plane and removal of layers, if any had infiltrated the epoxy fast-set. During the grinding process specimens were continuously rinsed with running water.

Upon completion of the grinding process, specimens were placed in an ultrasonic bath with distilled water to displace any lodged particles. Specimens were then polished for a total of 2 minutes with a microcloth impregnated with a colloidal silica polishing suspension, Buehler Mastermet, to achieve a surface roughness of 60 nm. After polishing, specimens were once again placed in the ultrasonic bath and then placed in a distilled water bath until the time of nanoindentation.

The designated indentation locations on the cement paste specimens were selected using a high magnification light microscope attached to the NanoTest TM 600 platform (1000X). Ten indentations were performed along a straight line spaced at 50 μm under a load of 1.0 mN. The indentation load was applied at a constant loading rate of 0.025 mN/second. Five indentations were selected to perform the fracture analysis.

3 ANALYTICAL METHODS

The analysis method is based on the energy approach originally introduced for ductile materials by Cheng et al. (2002). It is assumed that the fracture energy (U_{fra}) is accounted for as a portion of the irreversible energy, rather than total energy. The irreversible energy (U_{ir}) can be defined as the sum of the energy due to pure plasticity (U_{pp}) and the energy due to the extension of cracking (U_{crack}), described as

$$U_{ir} = U_{pp} + U_{crack} \tag{13}$$

The energy due to pure plasticity (U_{pp}) can be computed from the ratio of plastic to total energy

after Cheng et al. (2002).

$$\frac{U_{pp}}{U_t} = 1 - \left[\frac{\left[1 - 3\left(h_f / h_m \right)^2 + 2\left(h_f / h_m \right)^3 \right]}{\left[1 - \left(h_f / h_m \right)^2 \right]} \right] \quad (14)$$

where h_f is the residual indentation depth, h_m is the maximum indentation depth, and U_t is the total energy obtained from fitting a power law function to the loading portion of the indentation curve and substituting into Equation 5. The pure plastic energy (U_{pp}) can be found by multiplying the right hand side of Equation 14 by the total energy (U_t). Once the plastic energy is determined, the cracking energy can be determined from Equation 15.

$$U_{crack} = U_{ir} - U_{pp} \quad (15)$$

The critical energy release rate G_c can then be determined as

$$G_c = \frac{\partial U_{fra}}{\partial A} = \frac{U_{fra}}{A_m} \quad (16)$$

where A is the maximum crack area given for Berkovich indenter based on the maximum indentation depth by substituting h_{max} into Equation 2. Equation 16 assumes that the crack growth under nanoindentation load is stable. The fracture stress intensity factor K_c can be computed from the energy release rate (G_c) and reduced modulus (E_r) as

$$K_c = \sqrt{G_c E_r} \quad (17)$$

4 RESULTS

A typical load-indentation curve is shown in Figure 4. The results of five nanoindentation tests on the cement paste are summarized below in Table 1. Upon application of the analytical approach, the energy components are listed in Table 2. The final fracture parameters are listed in Table 3.

Table 1. Summary of five nanoindentation test parameters as extracted from the cement paste.

Test #	Maximum indentation depth h_m(nm)	Maximum indentation depth h_r(nm)	Reduced Elastic modulus E_r (GPa)
1	268	228	27.1
2	209	150	18.6
3	208	123	10.7
4	340	236	9.0
5	301	219	11.9

Table 2. Summary of five nanoindentation test energy component (nJ) as extracted from the cement paste experiments.

Test #	U_t	U_{pp}	U_e	U_{crack}
1	100.0	78.0	17.0	5.0
2	69.7	41.8	18.2	9.7
3	116.5	51.2	36.0	29.3
4	218.2	124.1	29.8	64.2
5	307.1	188.2	98.3	20.6

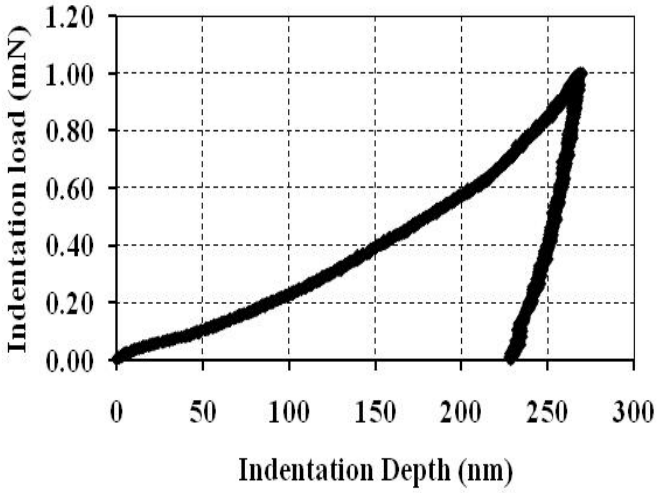

Figure 4. Typical load-indentation curves for nanoindentation of the cement paste.

Table 3. Fracture parameters G_c and K_c of cement paste as extracted from nanoindentation.

Test #	G_C (N m/ m^2)	K_C (MPa m$^{1/2}$)
1	2.8	0.278
2	9.0	0.409
3	27.7	0.544
4	22.7	0.453
5	9.3	0.332
Mean	14.3	0.403
Standard deviation	±10.4	±0.104

5 DISCUSSION

The proposed method was able to extract the fracture toughness of cement paste. Comparing the observed results to macroscale observations might provide some insight on the scale effect. Experiments by Shah (1988) on cement paste showed fracture toughness of cement paste ranges between 0.3-0.5 MPa m$^{1/2}$ which is similar to the range of fracture toughness values extracted from the nanoindentation experiments. While the fracture toughness values extracted here reasonably compare to values from the literature, a wide scatter in the fracture characteristics extracted from nanoindentation can be observed. This scatter is represented by the relatively high standard deviation is and can be attributed to the limited number of indentations reported here (5 indentations).

It is important to note here that for a quasi-brittle material such as cement paste a single radial crack as in metals would not develop. Instead many nanocracks would develop in the fracture process zone. Therefore, the proposed method assumes an equivalent elastic radial crack to simulate the energy consumed in the fracture process zone. This assumption is in line with quasi-brittle fracture mechanics assumptions suggested by many researchers to model cemetitious materials (e.g. Karihaloo and Nallthambi 1989, Shah et al. 1995). The effect of any inelasticity is assumed negligible.

It is also obvious that nanoindentation of the cement paste can result in indenting any of the cement paste phases including high and low density CSH, calcium hydroxide (CH), ettringite, pores and unhydrated cement. The fact that the phase indented cannot be determined *a priori*, results in the difficulty to relate the fracture toughness observations to a single phase in cement. However, statistical analysis of nanoindentation data proposed by Constantinides & Ulm (2004) showed that for a limited number of indentations, most of the observed characteristics can be related to CSH due to the relatively large volume fraction of CSH in cement paste. Phase correlation with certainty requires knowledge on the mechanical properties of CSH tested independently of other phases. This information is not widely available.

We further compared the fracture toughness results described above with those extracted using an alternative approach for extracting the fracture toughness from nanoindentation experiments suggested by Cheng et al. (2002). In this alternative approach, the fracture toughness parameters are determined with the aid of the finite element method. The alternative approach assumes that the cracking energy is part of the total energy observed during nanoindentation such that

$$U_t = U_p + U_e + U_{crack} \qquad (17)$$

Therefore, if an elastic-plastic constitutive model is used to simulate the load-indentation response using the finite element method, the cracking energy can be based on the difference in energies between experimental data and finite element simulation. A finite element model for simulating Berkovich nanoindentation is shown in Figure 5. The finite element model exploits the one third symmetry of the Berkovich indenter for computational efficiency. Four-node solid 45 elements are used to model the plastic behavior of the nano-indentation process. Material properties were determined iteratively so that the load-indentation simulated by the finite element method meets that observed experimentally in Test # 1. Materials properties include a Young's modulus of elasticity of 110 GPa, a yield stress of 50 MPa and yield strain of 0.0045 nm/nm and Poisson's ratio of 0.25. The model implements non-linear Newton Raphson method for convergence.

The results of the alternative approach showed that both curves observed experimentally and extracted from the finite element model were approximately the same. Figure 6 shows the load-indentation curves as extracted from the finite element model in comparison with that observed experimentally. No major difference in the energy absorbed extracted from the finite element model and that of the experiments can be observed. While part of the finite element loading curve came above the experimental loading curve, another part came below the experimental curve. The difference in energy resulted in a cracking energy U_{crack} of 7.42 nJ and therefore in a fracture toughness K_c of 0.338 MPa $m^{1/2}$ compared with 0.278 MPa $m^{1/2}$ using the proposed method.

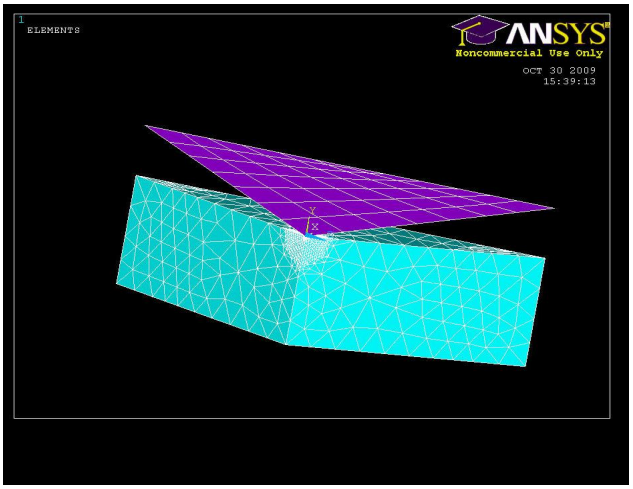

Figure 5. The finite element model simulating Berkovich indentation of Test #1.

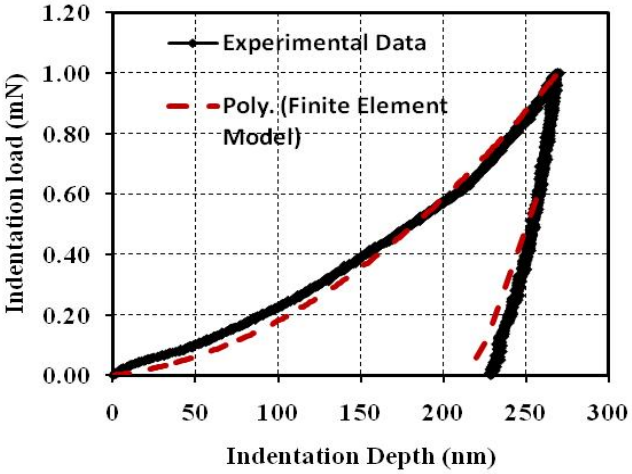

Figure 6. Comparison between load indentation simulated using the finite element method and observed experimentally.

The alternative method, therefore, was not able to fully verify the results extracted from the proposed method. While the numerical value of the fracture toughness extracted from the alternative method is

within range compared to the fracture toughness extracted from the proposed method, the difference in the loading curve is within experimental accuracy. The results therefore are not conclusive. Further research is still warranted to confirm and refine the above methods. Nevertheless, it is obvious that nanoindentation can provide a plethora of information on fracture of cementitious composites while avoiding the complexity associated in performing macroscale fracture toughness experiments.

6 CONCLUSIONS

Fracture toughness parameters of cement paste specimens made of 0.5 water/cement ratio was determined using nanoindentation. The proposed method is based on decomposing the plastic energy to pure plastic energy used in producing the irreversible indentation and cracking energy that helps crack propagation. An equivalent elastic radial crack is assumed and the energy required to extend this crack is computed. The cracking energy is computed using the experimentally observed nanoindentation loading and unloading curves. The proposed method avoids the need to measure radial cracks which proved difficult with cementitious composites. The fracture toughness parameters were found to be in range with macroscale fracture toughness of cement paste reported in the literature. Further research is underway to validate the proposed method and to classify the fracture contributions of the different phases in the cement paste.

ACKNOWLEDGEMENTS

The authors greatly acknowledge the financial support to the graduate students by Defense Threat Reduction Agency (DTRA) Grant # HDTRA1-08-1-0053. The support of the National Science Foundation through the Nanotechnology Undergraduate Education (NUE) grants # 0936412 and 0741525 is greatly appreciated.

REFERENCES

Anstis G.R., Chantikul, P., Lawn, B.R. & Marshall, D.B. 1981. A critical evaluation of indentation techniques for measuring fracture toughness: I, Direct crack measurements. *Journal of American Ceramics Society* 64:533–538.

Chen, J. & Bull, S.J. 2007. Indentation fracture and toughness assessment for thin optical coatings on glass. *Journal of Applied Physics* 40:5401–5417.

Cheng, Y.T., Li, Z.Y. & Cheng, C.M. 2002. Scaling, relationships for indentation measurements. *Philosophical Magazine A, Physics of Condensed Matter Structure, Defects and Mechanical Properties* 82:1821–1829.

Constantinides, G. & Ulm, F.J. 2004. The effect of two types of c-s-h on the elasticity of cement based materials: results from nanoindentation and micro modeling. *Cement and Concrete Research* 34:67–80.

Dukino, R.D. & Swain, M.V. 1992. Comparative measurement of indentation fracture toughness with Berkovich and Vickers indenters. *Journal of American Ceramic Society* 75(12):3299–3304.

Field, J.S., Swain, M.V. & Dukino, R.D. 2003. Determination of fracture toughness from the extra penetration produced by indentation-induced pop-in. *Journal of Materials Research* 18(6): 1412–9.

Fisher-Cripps, A.C., *Nanoindentation*, Springer, New York, 2004.

Harding, D.S., Oliver, W.C. & Pharr, G.M. 1995. Cracking during nanoindentation and its use in the measurement of fracture toughness. *Materials Research Symposium*. Houston: 663–668.

Karihalloo, B. L., and Nallathambi, P., 1989. An Improved Effective Crack Model for the Determination of Fracture Toughness in Concrete. *Cement and Concrete Research*, 19: 603-610.

Kim, J. J., Fan, T., Reda Taha, M.M. 2010, A Homogenization Model Examining the Significance of Nanosilica on Concrete Strength and Stiffness. *Journal of the Transportation Research Board (TRB)*, in press.

Laugier, M.T. 1987. Palmqvist Indentation Toughness in WC-Co Composites. *Journal of Material Science Letters* 6:897–900.

Li, G.Y., Wang. P.M. & Zhao, X. 2007. Pressure sensitive properties and microstructure of carbon nanotubes reinforced cement composites. *Cement and Concrete Composites* 29(5):377–382.

Li, X., Diao, D. & Bhushan, B. 1997 Fracture mechanisms of thin amorphous carbon films in nanoindentation. *Acta Materialia* 45(11):4453–4461.

Mondal, P., Shah, S.P. & Marks, L. 2007. A Reliable Technique to Determine the Local Mechanical Properties at the Nanoscale for Cementitious Materials. *Cement & Concrete Research* 37(10):1440–1444.

Oliver, W.C. & Pharr, G.M. 1992. An improved technique for determining hardness and elastic modulus using load displacement sensing experiments. *Journal of Material Research* 7:1564–1583.

Reda Taha, M.M., Kim, J.J. Soliman, A., Sheyka, M. & Reinhardt, A. "Significance of Nanosilica on Fracture Toughness of CSH", *Materials and Structures*, in preparation.

Rosenfeld L.G., Ritter, J.E., Lardner, T.J. & Lin, M.R. 1990. Use of the microindentation technique for determining interfacial fracture energy. *Journal of Applied Physics* 67:3291–3296.

Scholz, T., Schneider, G.A., Muñoz-Saldaña, J. & Swain, M.V. 2004. Fracture toughness from submicron derived indentation cracks. *Applied Physics Letters* 84:3055.

Shah, S.P. 1988. Fracture toughness of cement-based materials. *Materials and Structures* 21:145–150.

Shah, S.P., Swartz, S.E., and Ouyang, C. *Fracture Mechanics of Concrete: Applications of Fracture Mechanics to Concrete, Rock and Other Quasi-Brittle Materials*, John Wiley & Sons Inc, New York, 1995.